Experimental Investigation of an Axisymmetric Turbofan Diffuser

Zachary M. Hall[1]
Aerospace Engineering, Auburn University Auburn, AL, 36849

Results of tests on an axisymmetric turbofan are presented to better describe the flow conditions and effect of the inlet diffuser's geometry on the diffuser's pressure recovery. The tests consisted of flow visualization using Laser Induced fluorescence, hydrogen bubbles, and Particle Image Velocimetry. Pressure gradients and streamlines were obtained for future comparison with computational modeling of the same test configurations.

Nomenclature

A_C	=	Capture Area
Ar	=	Capture Area
AOA	=	Angle of Attack
CAR	=	Capture Area / Fan Face Area
CFD	=	Computational Fluid Dynamics
Cp	=	Pressure Coefficient
m	=	mass flow rate
Re	=	Reynolds Number based on fan blade diameter
u	=	velocity
ρ	=	density
∞	=	freestream

I. Introduction

For this effort the geometry used is that of the CFM56-5B turbofan inlet duct. The CFM56 engine is a single stage turbofan engine designed for broad range of commercial and military aircraft and first entered into service in 1974. The CFM56-5B has the highest fan pressure ratio of all CFM56 engines, providing between 22,000 and 33,000 lbs of thrust, and is the first commercial engine to use an ultra-low emissions combustor. It first entered service in 1994 when used on an Airbus A321 passenger plane. It currently powers the twin-engine Airbus A318, A319, A320, and A321 airplanes.

Computational fluid dynamics (CFD) is a rapidly maturing field and as computational methods improve and with increasing computing power, computational times will continue to decrease, thus making it an attractive method of flow prediction. CFD can provide computational results that appear to accurately model complex flow fields. However, computational models still must have it's the accuracy justified by experimental data or other validated computations to be considered valid. Expensive experimental techniques such as the water tunnel and wind tunnel testing are regularly complemented by CFD results for test planning.

Particle image velocimetry (PIV) and laser induced fluorescence (LIF) are two common flow visualization techniques used to compare to computational results because of their ability to obtain velocity measurements non-invasively. PIV is used primarily to obtain quantitative data in the form of flow statistics (velocity, vorticity etc.), while LIF is used to obtain qualitative data in the form of streamlines.

The purpose of this effort is to obtain experimental data for the axisymmetric turbofan inlet design to compare with computational results. Once CFD results have been found to correctly model real world conditions by being close to the experimental results, the computational assumptions can be said to be validated. Future works will vary the geometry of the inlet using genetic algorithms in an effort to improve flight characteristics. In the past, genetic algorithms have been used for the optimization of aerodynamic shapes for freight trucks[1], gas turbine engines[2], missiles[3], and aircraft wings and airfoils[4,5], and combustors[6].

[1] Graduate Student, Aerospace Engineering, student member, AIAA.

II. Model Geometry

The axisymmetric model's geometry was determined from available CFM56-5B specifications using genetic algorithms[7]. From the 2-D engine airflow geometry available, Figure 2, four equations were found to represent the four surfaces of the duct. Bernstein polynomials have been proven to accurately represent airfoils and nacelles[7]. A real-coded genetic algorithm was used to randomize these Bernstein polynomials to match twenty points obtained from the figure for each curve. Four equations were found, with a percent difference from the data points to match less than 0.1 %, which was assumed to be a negligible error.

An axisymmetric model was chosen over the real world non-axisymmetric CFM56-5B geometry due to machining limitations using a CNC lathe. The upper 2-D cross section of the CFM56-5B geometry was chosen to revolve 360º to create the axisymmetric model used for this effort. A comparison of the model geometry used and the CFM56-5B is presented in Figures 1 & 2. The upper section was chosen because it had a greater camber than the lower section and because the lower 2-D cross section is more blunt which was assumed to be to be designed for low ground clearance on A319's. It was determined that the upper 2-D geometry section was more critical to the design optimization for cruise conditions.

The model was made of acrylic to permit light to shine through the model to be able to get flow visualization and PIV data on the inside of the model cavity. Initially after machining, the model had a turned finish and was somewhat opaque. The model was polished using NOVUS polish remover level 2 and then level 1.

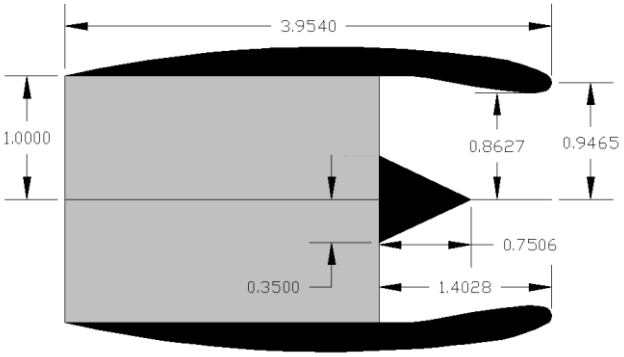

Figure 1. Axisymmetric Model Dimensions (inches)
Reversed Orientation presented here

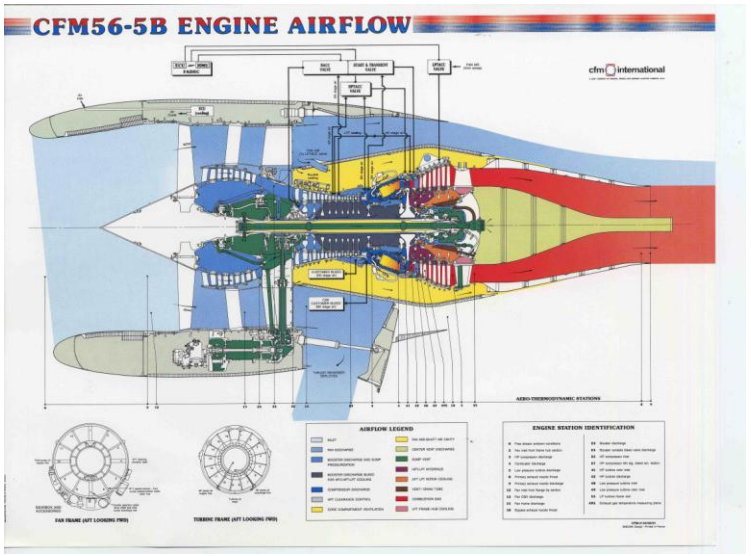

Figure 2. CFM56-5B Duct and Engine Layout.
Photos courtesy of CFM International, a 50/50 joint company between Snecma (SAFRAN Group) and General Electric Company

III. Experimental Setup

All PIV tests were conducted in the Auburn University Aerospace Engineering 45 cm x 45 cm cross-section test section water tunnel. The test section was 2 m long and transparent, which allowed for flow visualization and PIV measurements. The water tunnel was capable of maximum velocity of 1.1 m/s and had a turbulence intensity of 1% at maximum velocity. The tunnel was run at Reynolds numbers of 17600, 46540, 61160, and 90400, with the characteristic length being the fan diameter.

In the water tunnel the model was sting mounted in a specially designed support system that was connected to a constant volumetric flow rate water pump to achieve a favorable pressure gradient in the cavity of the model. This was to simulate the fan drawing air into the engine to be combusted for thrust generation in real world conditions. This extracted flow was deposited back into the water tunnel through a hose, at approximately thirty times the body diameter behind the model support system, which was assumed to have a negligible effect on the flow field. A vertical support was attached to the sting mount at approximately four body diameters behind the trailing edge of the model. The support system rested on the top of the tunnel walls. This distance was chosen to limit the moment arm caused by the model on the support system, while also minimizing disturbance caused by the cylindrical vertical support strut. The mass flow rate was determined from the measured volumetric flow rate using a Fill-RITE digital flow meter attached directly after the rate water pump. A 2-D laser sheet was created using an argon laser and reflected using a mirror below the tunnel onto the model as can be seen in Figure 3. The laser sheet was set at an obtuse angle to prevent shadows caused by refraction in the leading edge of the lower surface from being present in the PIV images.

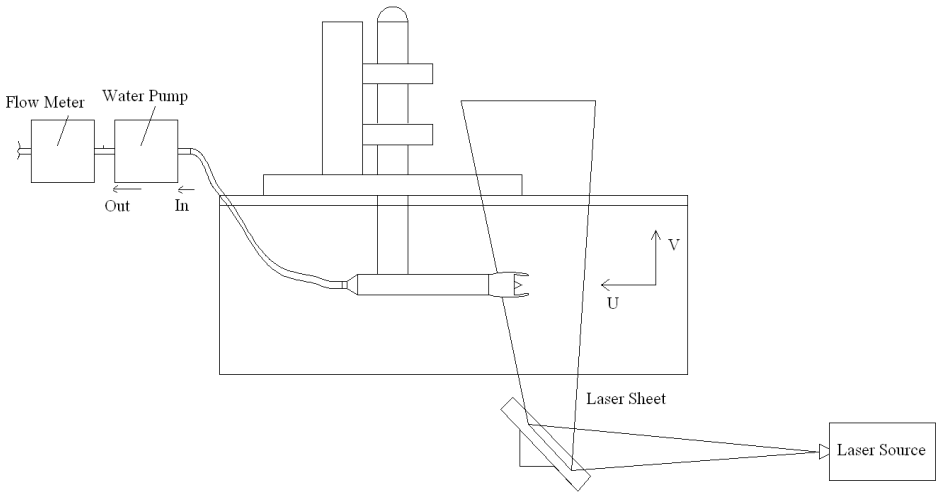

Figure 3. Water Tunnel Mounting System & Laser Setup

Hydrogen bubble wire and LIF was used in this effort, simultaneously and alone. Hydrogen bubbles were produced by applying voltage across a platinum wire and anode to create a sheet of bubbles. The voltage caused electrolysis which caused the hydrogen and oxygen in the water to separate and form visible hydrogen bubbles that follow fairly accurately the path of the flow. A 2mm thick beam light sheet was positioned to illuminate the bubbles. (The bubbles were seen by the camera by illuminating them with a laser placed tangent to the plane of the bubbles.) A constant voltage of 34 V was applied through the probe for all tests as it had been seen to create the optimum size and amount of bubbles for flow visualization. A vertical bubble wire probe was used to obtain data on the X-Y plane. The probe consisted of three equally spaced 32 Swg platinum wires. The probe was mounted onto a traversing system that rested on the tunnel side walls, which enabled specific placement of the probe[9].

For the LIF tests, a solution of sodium flourescein salt was injected into the freestream flow at approximately two model body diameters away from the leading edge of the nacelle model. Flow visualization results were recorded using a camera. The video records were post processed using a JVC professional player. Selected images were printed using a Sony video printer.

"A Dantec Dynamics PIV system, consisting of a New Wave Research 50 mJ dual-pulse ND: YAG laser, a Highsense 1k x 1k cross-correlation CCD camera and a PIV 2100 processor, was used to acquire PIV images that were processed using Dantec Flow Manager Software."[9]

The flow was seeded with highly reflective silver coated hollow plexi-glass with a nominal diameter of 20 micrometers. The flow was illuminated with two consecutive laser pulses, with the time between each pulse varied according to the freestream Reynolds number. PIV images were statistically averaged from 50 pairs of images. The interrogation window was 32 pixels x 32 pixels.

IV. Flow Conditions

The CFM56-5B turbofan engine is primary engine for the Airbus A319. The cruise conditions to match were assumed to be equal to the A319's cruise conditions, where are as follows: M = 0.8, altitude = 13000 m, and the mass flow rate at sea level is 900 pounds per second. A mach number of 0.8 is unattainable in the subsonic incompressible water tunnel, so another method of flow similarity needed to be used. The method chosen f or in the water tunnel was to match the ratio of the free stream velocity to the velocity at the fan face at cruise conditions. The velocity at the fan face in real world conditions was calculated from the known mass flow rate of 900 pounds per second at sea level. The mass flow rate at cruise altitude was determined by the using the density ratio of sea level to cruise altitude.

$$mdot_{altitude} = \frac{\rho_{altitude}}{\rho_{SL}} mdot_{SL} \tag{1}$$

From the mass flow rate at cruise, the velocity was obtained using the continuity equation.

$$A = \frac{mdot}{\rho_{\infty} * v_{\infty}} \tag{2}$$

The ratio of the free stream velocity to the velocity at the fan face for cruise was calculated to be approximately equal to 0.5. To ensure any errors caused by assumptions did not significantly affect the results, the free stream Reynolds number was varied above and below the calculated Reynolds. This ensured that all of the major trends of the flow were recorded.

The mass flow rate of the water tunnel model fan face was recorded to be 6.45 gpm, or .897 lb/s. The velocity at the fan face was determined to correspond to a Re of 45000.

V. Results and Discussion

a. Flow Visualization Results

The bubble wire technique was efficient at showing the major trends of the flow, especially capture area and spill over. The LIF was an efficient method for visualizing the flow inside and outside of the model by visualizing the streamlines of the flow. However, a disadvantage was that turbulence was introduced into the flow due to the wake of the cylindrical dye injection tube. Counter-rotating vortices formed in the wake of the cylinder in the flow can be seen in Figure 4. It was assumed that the major trends of the flow were not too adversely affected by the introduced turbulence.

As Reynolds number increased, the CAR decreased, Figures 5 & 7. This was made evident by the streamlines of dye injected at the same vertical position upstream of the model. As the Reynolds number increased the streamlines diverged more greatly from the centerline of the model. It was assumed that the larger adverse pressure ratio due to increased freestream velocities caused this effect. This can be attributed to the fact that as the freestream Reynolds number increased, the freestream pressure decreased, while the pressure at the fan face stayed constant because of the flow. To better understand the phenomenon it can be imagined that instead of lowering the pressure in the freestream, the pressure was increased at the fan face, thus matching the same pressure ratio.

The maximum possible CAR occurs when the freestream velocity is equal to zero, which can be imagined to be at take off conditions in ground effect, Figure 8. The bottom surface of the water tunnel can be seen in the image. The capture area is so large that even streamlines tangent to the horizontal line of the model can be seen to travel into the model and become tangent to the surface of the nose cone.

b. PIV Results

Cp gradients were determined for each condition using Bernoulli's equation by assuming that the total pressure of the flow remained constant, equation 3.

$$Cp = 1 - \frac{v}{v_\infty} \tag{3}$$

Qualitative data is presented in the form of streamlines and quantitative is represented by the gradient plots on each figure. The CAR was determined from the streamlines. Cp gradients were over-layed on the same plots to show the effect of capture area on static pressure. The Reynolds number was varied from 25% to 150% of the calculated freestream Reynolds number, at increments of 25% to obtain PIV results for all similar flight conditions; when the CAR was less than one, approximately equal to one, and greater than one.

The area capture ratio was approximated for each test condition by setting the capture area as when the streamlines were approximately at an AOA equal to the AOA of the model. The trend of the CARs decreasing as Reynolds numbers increased is presented in Figure 18. A CAR approximately equal to one was determined to be when the Reynolds number was 75% of cruise, corresponding to Cp values of zero at the leading face of the model, Figures 10 & 12. The streamlines outside of the radius of the model remained close to horizontal and were not greatly affected by the model. Also presented in these figures is the increased pressure caused by stagnation and bifurcation of the flow near the leading surface of the nacelle by slightly positive Cp values. Increased pressure due to bifurcation was not seen at other recorded Reynolds number conditions. This can be attributed to at larger or small Reynolds numbers the magnitude of Cp gradients being stronger near the surface of the model, minimizing or amplifying this effect. The purpose of the diffuser is to increase pressure at the fan face to improve thrust performance; therefore a CAR equal to one would not be an optimal cruise condition.

A CAR was less than as one was visualized at the calculated Reynolds number, shown in Figures 11& 13 with positive Cp values. The streamlines diverged greatly from the horizontal compared to CAR equal to one conditions. Increasing the Reynolds number past cruise caused the positive Cp values increase in magnitude and the streamlines to diverge even further. The pressure at the fan face would be greater when compared to cruise which would better fulfill the purpose of the diffuser, but it was understood that higher Reynolds numbers may approach the limit of the fan intake and would cause the model to become similar to a cavity and have re-circulating flow. A Reynolds number of approximately equal to 90,000 appears to approach this limiting Cp value, as can be witnessed in Figure 17. Future efforts to conduct PIV testing of the inside of the model hope to numerically determine this limit.

Inversely, a capture area greater than one was determined for Reynolds number equal to 25% the cruise condition Reynolds number, made evident by negative Cp values at the leading face of the model. The horizontal streamlines that originate above and below the radius of the nacelle travel into the leading face of the model. This can be imagined to be similar to transient take-off or landing conditions.

The angle of attack was also varied from zero to three degrees. It was determined that when at a positive angle of attack, more flow entered the model at the upper surface while oppositely less flow entered the model at the lower surface, as made evident by the streamlines. However, the total CAR at angle of attack remained constant compared to zero degrees angle of attack. It is understood that eventually a higher angle of attack would cause the flow entering the lower surface of the model would separate and cause recirculation. Future efforts to ascertain PIV results for the inside of the model hope to see this trend.

In conclusion Cp is directly proportional to Reynolds number and the CAR is inversely proportional to Reynolds number.

VI. Appendices

a. Laser Induced Fluorescence Flow Visualization Images

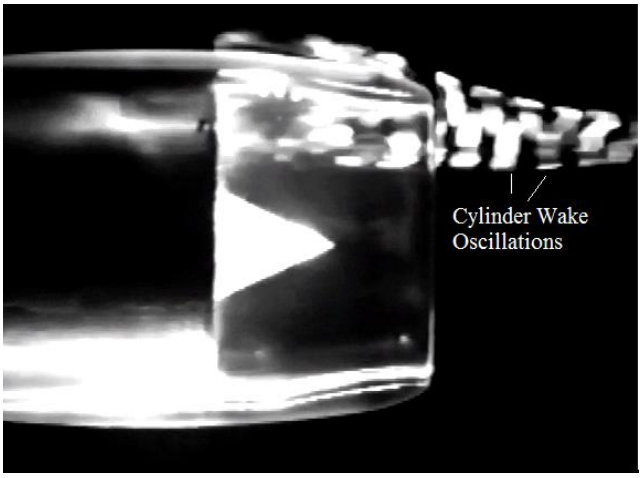

Figure 4. LIF AoA = 0º Re = 61160
Slight flow spillover at the upper surface

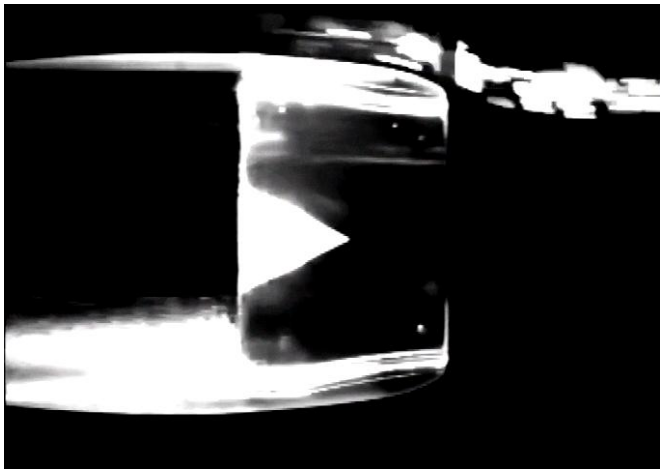

Figure 5. LIF Over AoA = 3º Re = 75780
Complete flow spillover at the upper surface

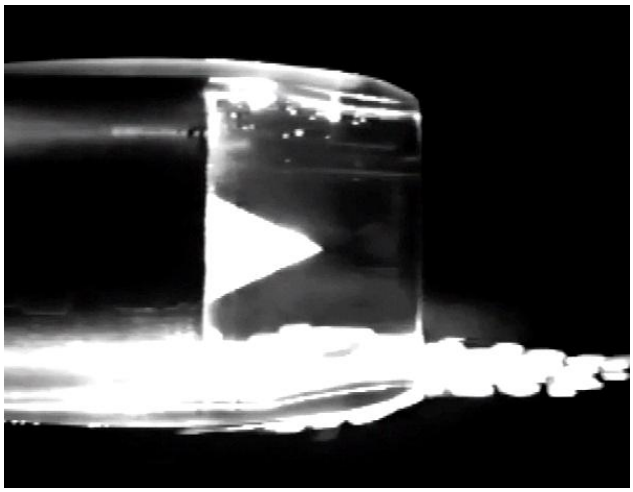

Figure 6. LIF AoA = 0º Re = 61160
Slight flow spillover at the lower surface

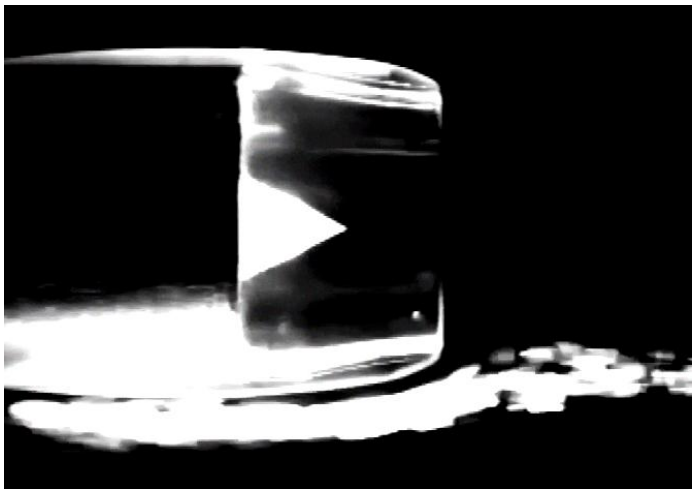

Figure 7. LIF AoA = 3º Re = 75780
Complete flow spillover at the lower surface

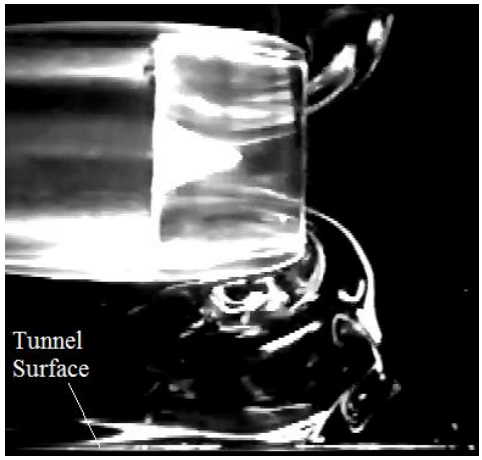

Figure 8. Ground Effect LIF A0A = 0 Re = 0 in
Maximum capture area in ground effect

b. Particle Image Velocimetry Images

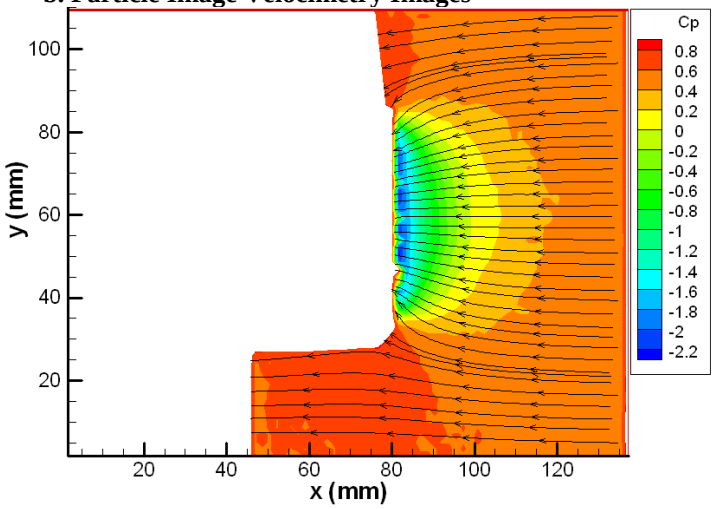

Figure 9. PIV AoA = 0º Re = 17600

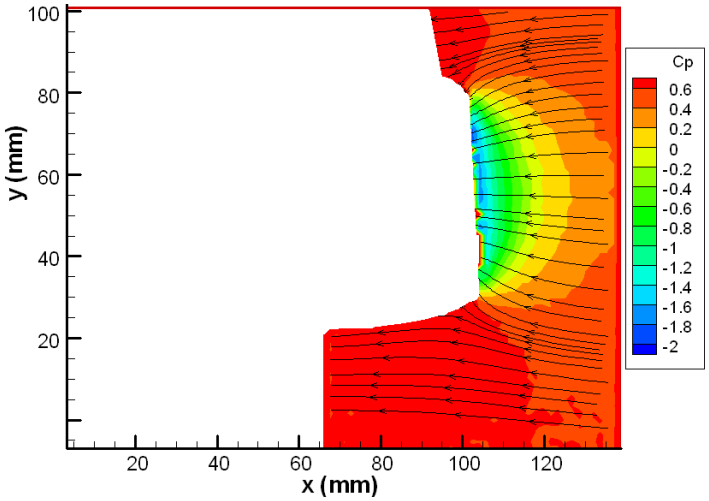

Figure 10. PIV AoA = 0º Re = 17600

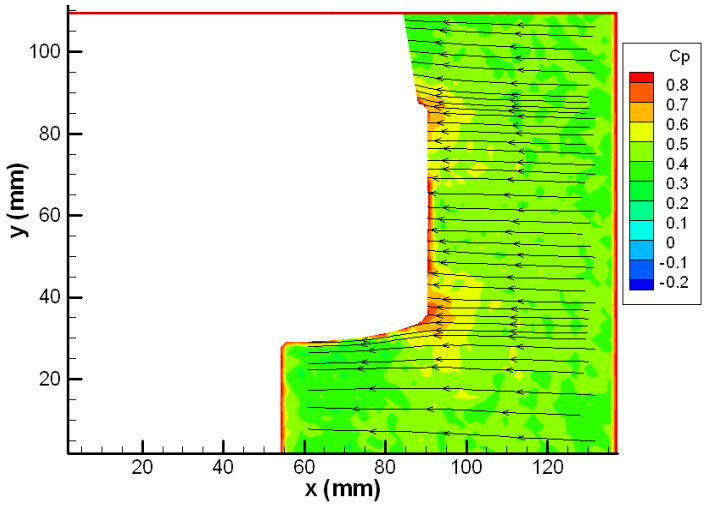

Figure 11. PIV AoA = 0º Re = 46530

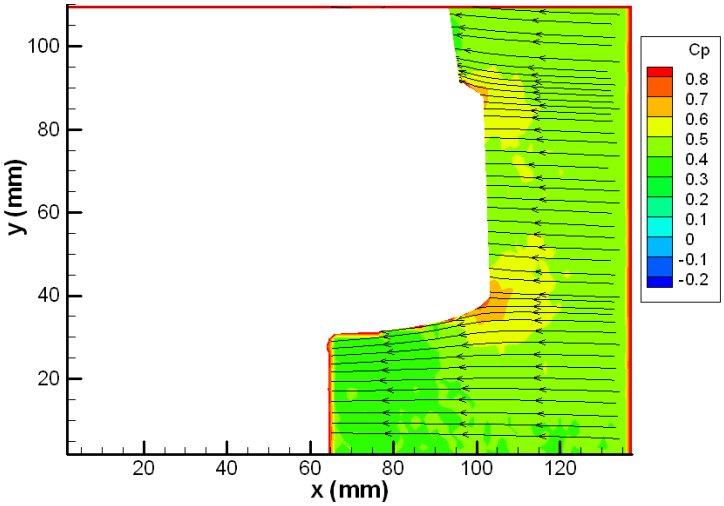

Figure 12. PIV AoA = 0º Re = 46530

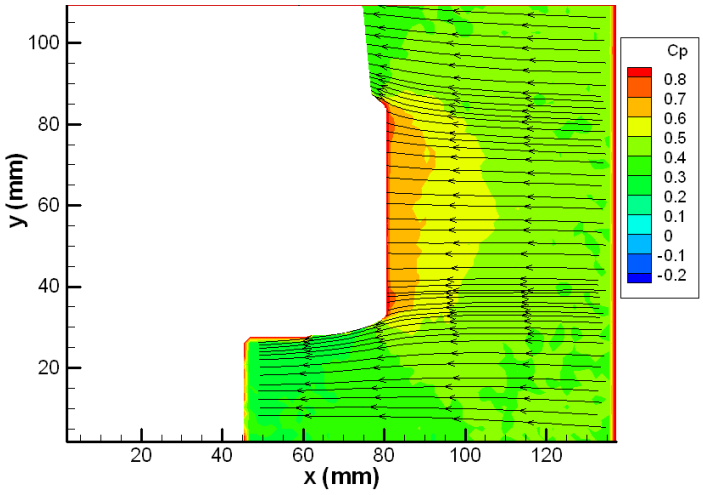

Figure 13. PIV AoA = 0º Re = 61160

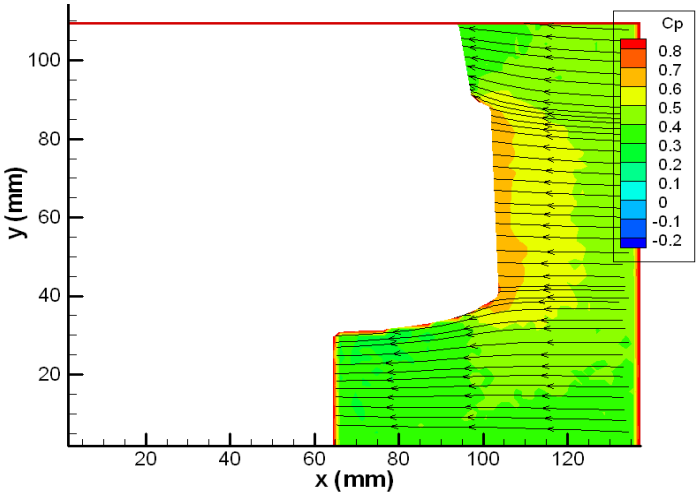

Figure 14. PIV AoA = 3º Re = 61160

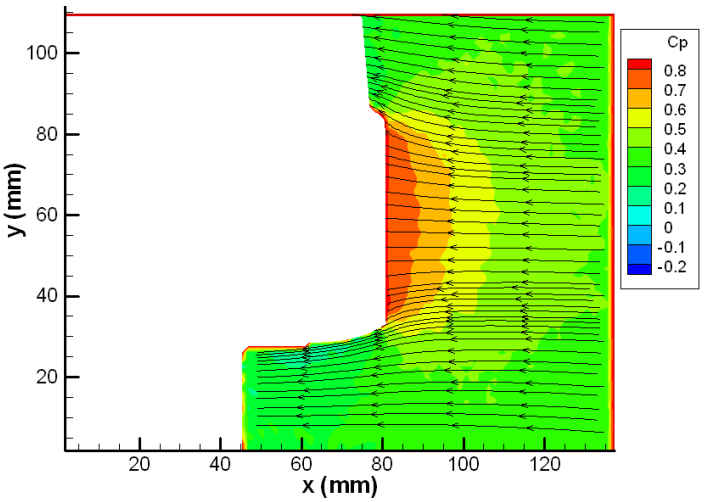

Figure 15. PIV AoA = 0º Re = 90400

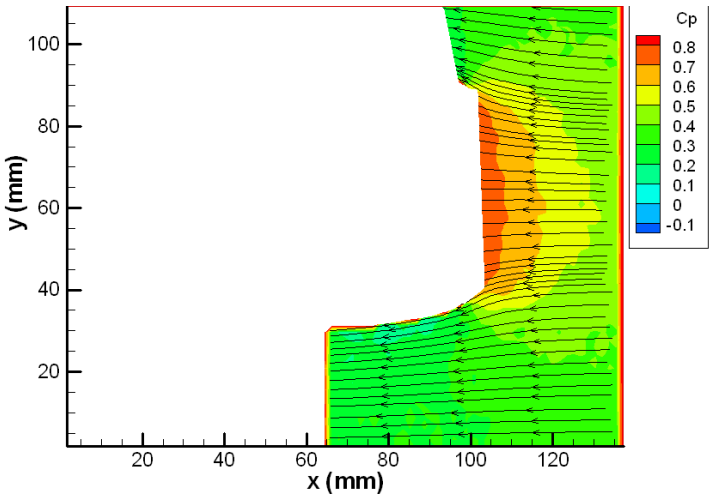

Figure 16. PIV AoA = 3º Re = 90400

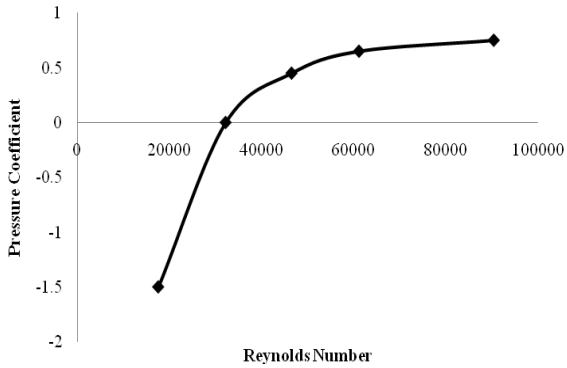

Figure 17. Leading Face Cp versus Reynolds Number

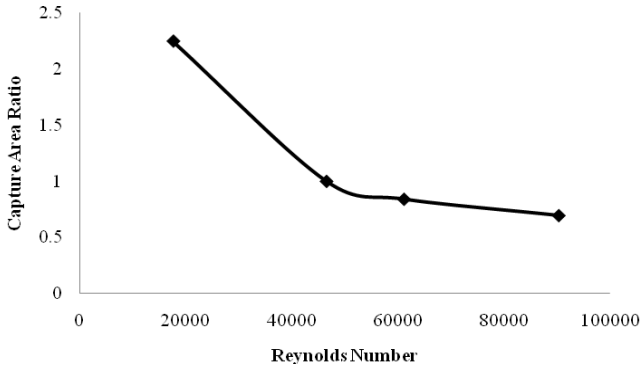

Figure 18. CAR versus Reynolds Number

VII. References

1. Doyle, J.,Hartfield, R.J., and Roy, C. *"Aerodynamic Optimization for Freight Trucks using a Genetic Algorithm and CFM"*, AIAA 2008-0323, presented at the 46th Aerospace Sciences Meeting and Exhibit, Reno, NV, January 2008.

2. Torella, G., Blasi, L., "*The Optimization of Gas Turbine Engine Design by Genetic Algorithms"*, AIAA Paper 2000-3710, 36th AIAA/ASME/SAE/ASEE Joint Propulsion Conference and Exhibit, July 2000.

3. J.E. Burkhalter, R.M. Jenkins, and R.J. Hartfield, M.B. Anderson, G.A. Sanders, *"Missile Systems Design Optimization Using Genetic Algorithms"*, AIAA Paper 2002-5173, Classified Missile Systems Conference, Monterey, CA, November, 2002

4. Anderson, M.B., *"Using Pareto Genetic Algorithms for Preliminary Subsonic Wing Design"*, AIAA Paper 96-4023, presented at the 6th AIAA/NASA/USAF Multidisciplinary Analysis and Optimization Symposium, Bellevue, WA, September 1996.

5. Perez, R.E., Chung, J., Behdinan, K., *"Aircraft Conceptual Design Using Genetic Algorithms"*, AIAA Paper 2000-4938, presented at the 8th AIAA/USAF/NASA/ISSMO Symposium on Multidisciplinary Analysis and Optimization, Bellevue, WA, September 2000.

6. Ahuja, V., *"Optimization of Fuel-Air Mixing for a Scramjet Combustor Geometry using CFD and a Genteic Algorithm"*, Master's Thesis, Auburn University, Alabama, Dec. 2008.

7. Kulfan B., M., *"A Universal Parametric Geometry Representation Method – CST"*, 45th AIAA Aerospace Sciences Meeting and Exhibit, 8-11 January, Reno, Nevada, 2007.

8. Hall, Z. "*Optimization of a Turbofan Inlet Duct using Genetic Algorithms and CFD"*, AIAA Applied Aerodynamics Conference submission, San Antonio, TX, June 2009

9. Rifki, R "*Flow Around Axisymmetric and Two-Dimensional Forward Facing Cavities*", Master's Thesis,Auburn University, Alabama May 2006

10. Vincenti, I., *"PIV Study for the Analysis of Planar Jets in Cross-Flow at Low Reynolds Number,"* University "Roma TRE" Rome (Italy)

11. Yigang, S.*, "Comparison of Six CFD Models for Room Airflow Study with PIV Measurement Data,"* ASAE/CSAE Meeting Presentation, Ontario, Canada, August 2004